



HAL
open science

Experimental analysis of hybrid energy storage system based on nonlinear control strategy

Youcef Oubbati, Brahim Khalil Oubbati, Abdelhamid Rabhi, Salem Arif

► To cite this version:

Youcef Oubbati, Brahim Khalil Oubbati, Abdelhamid Rabhi, Salem Arif. Experimental analysis of hybrid energy storage system based on nonlinear control strategy. *Revue Roumaine des Sciences Techniques. Serie Électrotechnique et Énergétique*, 2023, 68 (1), pp.96-101. 10.59277/RRST-EE.2023.68.1.16 . hal-04102168

HAL Id: hal-04102168

<https://u-picardie.hal.science/hal-04102168v1>

Submitted on 22 May 2023

HAL is a multi-disciplinary open access archive for the deposit and dissemination of scientific research documents, whether they are published or not. The documents may come from teaching and research institutions in France or abroad, or from public or private research centers.

L'archive ouverte pluridisciplinaire **HAL**, est destinée au dépôt et à la diffusion de documents scientifiques de niveau recherche, publiés ou non, émanant des établissements d'enseignement et de recherche français ou étrangers, des laboratoires publics ou privés.



Distributed under a Creative Commons Attribution 4.0 International License

EXPERIMENTAL ANALYSIS OF HYBRID ENERGY STORAGE SYSTEM BASED ON NONLINEAR CONTROL STRATEGY

YOUCEF OUBBATI¹, BRAHIM KHALIL OUBBATI², ABDELHAMID RABHI³, SALEM ARIF¹

Keywords: Integral sliding mode control; Hybrid energy storage system; Photovoltaic system; Super-capacitor; Battery; PI control; Dc-microgrid.

In this paper, a nonlinear integral sliding mode control for a hybrid energy storage system (HESS) based stand-alone dc microgrid has been proposed and applied experimentally. This hybrid system comprises a PV, super-capacitor, and battery. A classical PI-based linear control strategy has been designed to control battery and super-capacitor systems based on decoupling the high and low-frequency components to estimate reference current. Since the frequent discharge during operation, super-capacitor power can reach the lowest value, affecting controller performance and making the system unstable. From the experimental result, a nonlinear Integral sliding mode control ISMC is performed as an inner loop controller to regulate battery and super-capacitor power. Also, the PI controller is implemented as an outer loop controller to regulate the dc-link. The proposed control approach is compared with the linear PI controller to improve life extension and minimize stress on the battery. As a result, the proposed control strategy has achieved high dynamic system performance.

1. INTRODUCTION

Renewable energy sources are becoming increasingly appealing for our daily load requirements. Photovoltaic systems have been widely used recently to produce electricity. Their use is increasing for many reasons, such as decreased classical energy sources (gas and oil), abundant availability, and eco-friendly aspects. The power production from the PV systems depends strongly on the number of solar irradiations. Also, due to the non-linearity behavior of the PV system, the maximum power point tracking controller is necessary to push the PV system to produce maximum power [1–4]. However, since the load demand and PV system are inconsistent, the PV system cannot satiate load demand alone. Hence, the battery storage system offers a promising opportunity to alleviate the issue of load demand.

Batteries are commonly implemented in a standalone PV power system to fulfill the power mismatch between the load and production. Moreover, due to the PV system's changing output and the load's intermittent high-power demand, batteries are encountering frequent deep cycles and irregular charging [5]. These drawbacks would increase the replacement cost of the battery and shorten the battery's lifespan. Super-capacitor-battery hybrid energy storage system (HESS) is thus a practical solution to reduce the capital cost of the battery, battery stress, and sizing.

The advantage of using the HESS with a standalone PV power system would be providing both power capacities and high energy to solve situations such as load variations and weather-changing conditions (irradiation and temperature). A control strategy is necessary for HESS to manage energy sustainability to the maximum extent, as it is the control structure that contains the power flow of the battery and the energy utilization [6,7]. In the literature many control strategies have been proposed for HESS for remote area power systems (RAPS) consisting of super-capacitor capacitor-battery and PV power systems.

The authors of [8] presented an optimal control structure for HESS with a PV system. This control strategy is fully

achieved using a low-pass filter and a fuzzy logic controller. In addition, the membership functions of the FLC are optimized by particle swarm optimization PSO to achieve optimal battery peak current reduction. The implementation complexity of this method is relatively high. In [9], a comprehensive study of HESS for standalone PV systems has been presented to review the state of the art. It discusses potential topologies that are suitable for improving the battery lifespan.

Moreover, a control strategy for Battery-Super-capacitor with a standalone PV power system is proposed [10]. This control strategy consisting of PI-based liner control has been suggested to enhance the battery lifespan and reduce stress. Nonetheless, the super-capacitor voltage has not been regulated. The obtained results have shown low performances. Another nonlinear control strategy for ESS with PV power system-based dc-microgrid has been used [11]. To reduce the limitations of a linear PI control strategy. The main advantage of this proposed control is the robustness and small region of stability.

This paper is based on nonlinear Sliding Mode Control with integral action to alleviate the stress on the battery and improve its lifespan. The proposed control strategy has been verified experientially based on the test bench to evaluate the ability of this controller concerning robustness and performance. Moreover, the performances of this controller have been compared with a classical PI controller using simulation to test the robustness of this controller under fast-changing irradiation. The experimental results show that the proposed controller strategy exhibits better performances when compared to a state-of-art PI controller in terms of lifespan and stress on the battery reduction.

2. CONTROLLING ESS WITH INTEGRAL SLIDING MODE CONTROL

Figure 1 depicts the suggested control technique closed loops (inner and outer) diagram. This approach of control seeks to reduce battery stress and extend battery life. In the inner loop, the dc-bus voltage (V_{dc}) was compared with a reference voltage (V_{ref}), and the error was given to the

¹LACoSERE Laboratory, University Amar Telidji of Laghouat, Algeria, E-mail: y.oubbati@lagh-univ.dz and s.arif@lagh-univ.dz

²LTSS Laboratory, University Amar Telidji of Laghouat, Algeria E-mail: i.oubbati@lagh-univ.dz

³MIS Laboratory, University of Picardie Jules Verne, Amiens, France E-mail: abdelhamid.rabhi@u-picardie.fr

proportional-integral (PI) controller. This controller generates the total current references (I_{tref}) based on the energy storage system. This current is separated into a low-frequency component (I_{LFCref}) and a high-frequency component (I_{HFCref}) as written hereafter:

$$I_{LFCref} = \text{lowpass filter}(I_{tref}), \quad (1)$$

$$I_{HFCref} = H_{tref} - I_{LFCref}. \quad (2)$$

The battery reference current is determined by the low-frequency component as follows:

$$I_{batref} = I_{LFCref}. \quad (3)$$

The reference battery current I_{batref} is compared with the actual battery current I_{bat} , and the error I_{baterr} is given to the ISM Controller. The ISMC creates the bidirectional dc-dc converter control law (u). This instruction instructs the PWM generator to create a switch corresponding to the dc-dc converter interfaced with the battery. Since to the slow dynamics behavior of the battery, the convergence of I_{bat} to its reference value I_{batref} is not ensured. Thereby, the uncompensated battery power is written as follows:

$$P_{batuc} = (I_{HFCref} + I_{baterr})v_{bat}. \quad (4)$$

Super-capacitor will adjust for this uncompensated battery power. As a result, the reference current of the super-capacitor is provided as follows:

$$I_{SCref} = \frac{P_{batuc}}{v_{SC}} = (I_{HFCref} + I_{baterr}) \frac{v_{bat}}{v_{SC}}. \quad (5)$$

I_{SCref} is compared with the actual SC current (I_{SC}), and the error is given to the ISMC. The ISMC generates the command (u). These duty ratios are given to the PWM generator to generate switching pulses corresponding to SC switches. Finally, to push the PV system to produce maximum power under fast-changing irradiation, we use the nonlinear controller (Integral Back-stepping sliding mode) for the MPPT application published recently in [3].

2.1 INTEGRAL SLIDING MODE CONTROLLER

The average model of the Bidirectional DC-DC converter is written as follows:

$$\begin{cases} \frac{d}{dt} i_L = \frac{1}{L} [v_{bat} - (1-u)v_{bus}] \\ \frac{d}{dt} v_{bus} = \frac{1}{C_{bus}} [(1-u)i_l - i_b] \end{cases}. \quad (6)$$

The sliding surface is considered as follows:

$$S = e + k_s \int e dt, \quad (7)$$

where e is the error between the actual current I and the reference value I_{ref} is given as :

$$e = I_{ref} - I. \quad (8)$$

To force the sliding surface to be zero. So, the derivation of sliding surface as:

$$\dot{S} = \dot{e} + k_s e = \dot{I}_{ref} - \frac{1}{L}(v_{bat} - (1-u)V_{dc}) + k_s (I_{ref} - I). \quad (9)$$

Integral sliding mode equivalent control:

$$u_{eq} = 1 - \frac{L}{V_{dc}} (v_{bat} - \dot{I}_{ref} - k_s (I_{ref} - I)). \quad (10)$$

The output signal control of the integral sliding mode controller is given as follows:

$$u = 1 - \frac{L}{V} (v - \dot{I} - k (I - I_{ref})) - k \text{sign}(S). \quad (11)$$

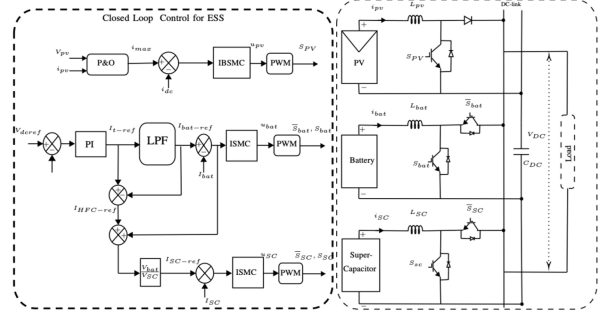


Fig. 1 – Structure of a stand-alone dc micro-grid with proposed control strategy.

The Lyapunov criteria have been considered in this work to prove the stability of the hybrid system. So, the candidate of the Lyapunov function is taken as follows:

$$V = \frac{1}{2} S^2. \quad (12)$$

By deriving this, Eq.12 gives as:

$$\dot{V} = S \dot{S}. \quad (13)$$

The stability is guaranteed if the derivative Lyapunov function is always negative. Form eq. 9 and 13, we can write:

$$\begin{aligned} \dot{V} &= S \dot{S} \\ &= (e + k_s \int e dt) \left(\dot{I}_{ref} - \frac{1}{L}(v_{bat} - (1-u)V_{dc}) + k_s (I_{ref} - I) \right) \end{aligned} \quad (14)$$

By putting Eq. 11 in Eq. 14

$$\dot{V} = S \left(\dot{I} - \frac{1}{L} \left(\frac{L}{V} (v - \dot{I} - k(e)) \right) V \right) + k(e) - \frac{V}{L} k \text{sign}(S) - \frac{v}{L} \quad (15)$$

Simplification of the last equation given as:

$$\dot{V} = S \left(-\frac{k_1 \text{sign}(S)}{L} \right) = -\frac{k_1}{L} |S| \quad (16)$$

where k_1 is a positive value.

3. BIDIRECTIONAL DC-DC CONVERTER MODELLING

The equivalent electric diagram of a bidirectional converter is shown in Fig 2. Converter switches ideally should transfer current in both directions to achieve reversibility of power flow. The first direction corresponds to the discharge mode. The converter transfers energy from the battery to the dc bus when there is a deficit in renewable energy production. The second represents the charging mode. When there is excess renewable energy production, the bidirectional converter transfers the excess dc bus

power to the battery. A bidirectional converter works as a boost converter during battery discharge and a buck converter during battery charging. This converter regulates the battery voltage in both modes (charge and discharge). dc bus controls the power flow.

$$\begin{cases} \frac{d}{dt} i_L = \frac{1}{L} [v_{bat} - (1-u)v_{bus}] \\ \frac{d}{dt} v_{bus} = \frac{1}{C_{bus}} [(1-u)i_L - i_b] \end{cases} \quad (17)$$

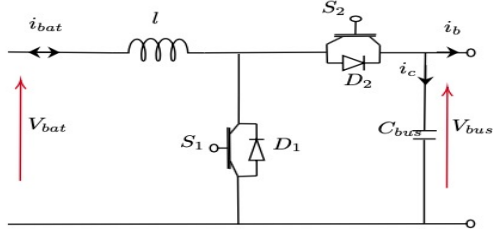


Fig. 2 – Equivalent bidirectional circuit.

The bidirectional converter we picked functions as a step-up converter to discharge and a step-down converter to charge the battery. The state model of this converter is obtained by taking the state vector, u , the converter command, and following the equation.

$$\begin{pmatrix} \dot{x}_1 \\ \dot{x}_2 \end{pmatrix} = \begin{pmatrix} 0 & -1 \\ 1 & 0 \end{pmatrix} \begin{pmatrix} x_1 \\ x_2 \end{pmatrix} + \begin{pmatrix} \frac{x_2}{L_1} \\ -\frac{x_1}{C_{bus}} \end{pmatrix} u + \begin{pmatrix} \frac{v_{bat}}{L_b} \\ -\frac{i_b}{C_{bus}} \end{pmatrix}. \quad (18)$$

The current exchanged with the DC bus may be expressed as follows using the rule of power conservation:

$$i_b = (1-u)i_{bat}. \quad (19)$$

4. SIMULATION RESULTS

The non-linear controller (ISMC) has been compared with a classical propositional-integral PI controller under changing weather conditions (Irradiation). The aim is to keep the dc-link voltage at the constant value $V_{dc} = 50$ V. The dc-link parameters are presented in Table 1. Moreover, the battery initial state of charge (SOC) equals 60 %. Table 2 shows the controller gains of strategy control inner and outer loop.

Table 1

Parameters of dc-link

Energy Sources & Converters	Parameters
2*PV system WU-120	MPP=120.7 W, $V_{oc} = 21$ V, $I_{sc} = 8$ A, $V_{max} = 17$ V, $I_{max} = 7.1$ A, array data (parallel = 4 and series = 2)
Battery SC	Lithium-Ion: $V_n = 24$ V, $I_c = 14$ A, SOC=60% $V = 40$ V, $C = 29$ f
Converters and DC-link	$L_{pv} = 0.352$ mH, $L_{bat} = 0.3$ mH, $L_{sc} = 0.36$ mH $C = 320$ uF, $V_{dc-ref} = 50$ V

As seen in simulation result, two cases are obscurely clear. The first case is the change in PV generation due to decreases in irradiation and increases in solar irradiation. At first, the PV system operated at maximum power using the MPPT controller [3] with an irradiation value equal to 1000 W/m^2 and a fixed temperature of $25 \text{ }^\circ\text{C}$. For figures can remark that:

Table 2

Parameters of controllers

Controllers	Gains
ISMC	$k_{s_{bat}} = 400, k_{i_{bat}} = 0.01,$ $k_{s_{sc}} = 2430, k_{i_{sc}} = 0.01$
	$k_{i_{dc}} = 3077, k_{p_{dc}} = 1.477, k_{s_{sc}} = 14800,$ $k_{p_{sc}} = 0.5, k_{i_{bat}} = 0.65, k_{p_{bat}} = 0.04$

For $[0 < t > 0.5]$ (case of constant irradiation), the PV supplies 980 W, and the load demand is 250 W. To conserve the surplus power of 730 W, between PV produced and load demand, the HESS intervened (charging the battery) to absorb it. In this case, the classical PI controller cannot guarantee the convergence load power at its reference value of 250 W. Moreover, the SC temporarily absorbs a high peak current of surplus demand with the current error of the battery. To ensure the convergence of the v_{dc} to its reference v_{ref} (see Figs. 3 and 4), this controller offered an overshoot and a slow settling time. However, in the case of using the ISMC, SC temporarily absorbs a high-frequency component of excess supply (see Figs. 7 and 8) owing to the slow dynamics of the battery. The battery current converges to a steady state slowly. Figure 6 shows that the increment in % SOC of the battery is less when compared to the PI controller.

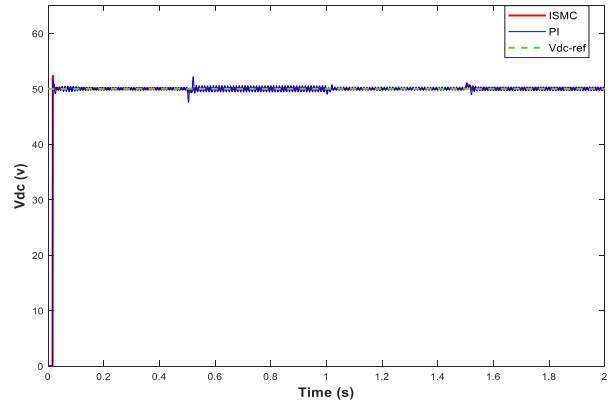


Fig. 3 – V_{dc} voltage (V) of the hybrid system in the case of PI and ISMC.

For $[1 < t > 1.5]$ (case of decreased Irradiation), the PV supplies 400 W, and the load demand is 250 W. The PV system works at maximum power using the same MPPT controller. Thereby, the different power between PV power and load demand ($250 \text{ W} - 150 \text{ W}$) is to be supplied (discharging) by HESS (see Figs. 7 and 8). Using a PI controller, the SC supplies a high-frequency component of excess demand momentarily. Also, due to the battery slow dynamics, battery power converges to a steady state slowly or suddenly decreases PV power, as depicted in Fig. 8. However, in the case of using the ISMC, the SC provides a high-frequency component of excess demand along with the battery error momentarily. To compare the performances of these controllers, the output powers are shown in Figs. 7 and 8. It shows that the PI controller cannot ensure the supply power to load required compared with ISMC. Figure 6 shows that increases or decreases in the % SOC of the battery is less when compared to the PI controller. Also, with the ISMC, the overshoot is reduced considerably, and the battery life is enhanced.

Moreover, the performance of the proposed controller (ISMC) and the classical PI controller can be compared based on various factors such as their ability to accurately track the reference, their global stability, their ripple

reduction, and their steeling time. Hence, from the obtained simulation results (see Fig. 4), the ISMC controller exhibits better performance with respect to the overshoot, the ripple reduction and the settling time.

Furthermore, the considered hybrid system is based on the PV connected with a battery and super-capacitor. Thereby, in such a system, the main drawbacks are the battery life and fast-tracking to the reference, and overshoot, in addition, to the battery dynamic behavior. All these factors inflation on the spin life of the battery and the dynamic performances of this hybrid system.

Finally, from obtained simulation results, the proposed controller has been achieved better dynamic performances compared to the classical PI controller in terms of ripples reduction, overshoot minimization, and fast settling time (see Figs. 4, 6, 7 and 8). These results suggest that the proposed controller may be a better choice for controlling such a system kind, at least under the specific operating conditions tested.

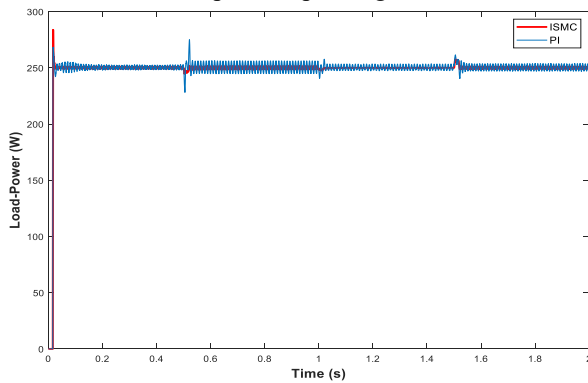


Fig. 4 – Load-power (W) of the hybrid system in the case of PI and ISMC.

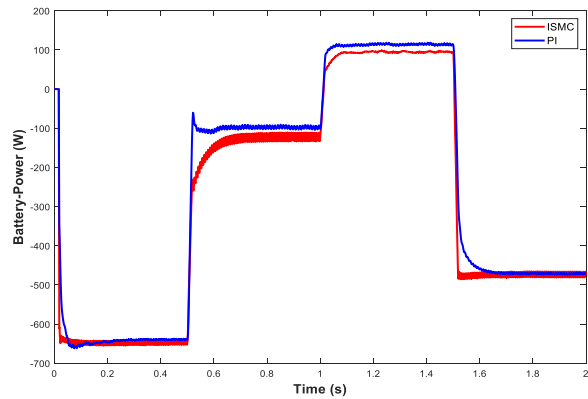


Fig. 5 – Battery-power (W) of the hybrid system in the case of PI and ISMC.

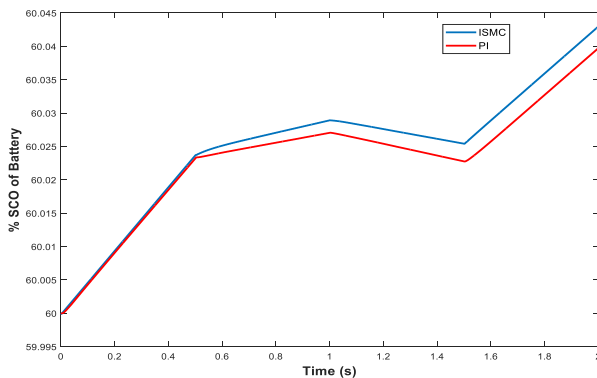


Fig. 6 – SOC of battery (%) of the hybrid system in the case of PI and ISMC.

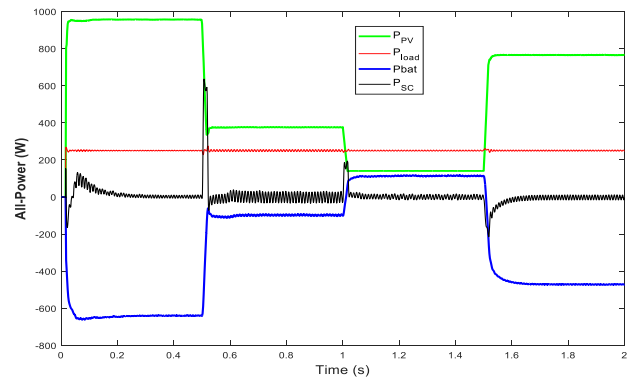


Fig. 7 – All-power responses of the hybrid system in case of PI controller.

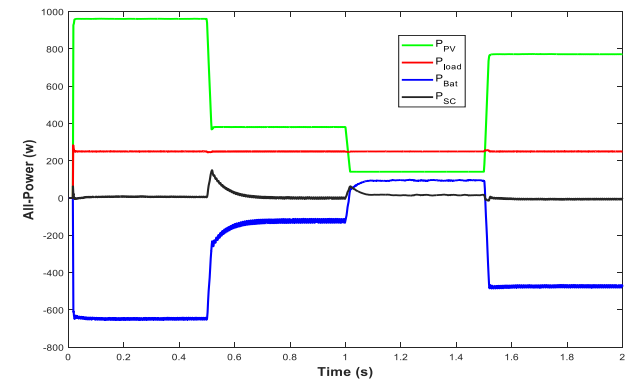


Fig. 8 – All-power responses of the hybrid system in case ISMC.

5. EXPERIMENTAL RESULTS AND DISCUSSIONS

To validate the simulation results. An experimental test bench was carried out in our laboratory (see Fig. 9), which consists of the following elements:

- dSPACE;
- Two Variable resistive load;
- Voltage and current sensors;
- Dc-dc boost converters;
- Bidirectional dc-dc converter for the super-capacitors;
- Bidirectional dc-dc converter for the battery;
- Two super-capacitors;
- Battery;
- PV module;
- Graphical user interface (GUI);

Moreover, the parameters for the used PV module are expressed in Table 3. In addition, the parameters of the dc/dc boost converters, the bidirectional dc/dc converter for super-capacitors, and the dc/dc converter for battery are given in Table 4.

Fig. 9 – Different required devices used for practical experience.

Table 3
Parameters of PV

Module Parameters	Value
Power at MPP P_{mpp} (W)	300
Short Circuit Current I_{sc} (A)	9.75
Voltage at MPP V_{mpp} (V)	31.9
Current at MPP I_{mpp} (A)	9.40
Open Circuit Voltage V_{oc} (V)	39.8
Module Yield η_M [%]	18.4

Table 4
Parameters of boost converter and controller.

Parameters	Value
k1	700
k2	8240.65
K3	0.01
K	1207
δ	0.5
Inductor, L (mH)	1
Capacitor, $C1$ (μ F)	200
capacitor, $C2$ (μ F)	2200
load resistor, R (Ω)	120

In this experience, we have tested the PV system-HESS connected with resistive load using the proposed nonlinear controller. To evaluate the effectiveness of the proposed controller strategy, we have considered two exams in this experience; firstly tested under constant reference value of DC-link and secondly under variable DC-voltage reference value, with real PV climatic condition for the both cases. The two experimental tests are described hereafter:

In this the first case: For $[0s < t < 2s]$, the performances of the nonlinear controller (ISMC) have been tested with constant reference value of DC voltage. The battery ensure the DC voltage regulation. In fact, the DC volatge is regulate to its reference value through the bidirectional DC/DC converter by using ISMC (see Fig.15). Moreover, from Figs (10 and 11) one can see that, the ISMC achieve better performance agninst the real PV irradiation change (see Figs.(10,11 and 12) at (0s to 0.1s)).

In the second case : For $[2s < t < 4s]$, in this case, the experiments were carried out by considering DC-volatge refernce vaule variation, in order to evaluate the abilty of the proposed controller in terms of rousteness, refernces tracking and goble system stability. From the obtained results, it can be seen evidently under reference value variation the ISMC is robust in the face of this variation which corresponds to charge and/or discharge of the super-capacitor and ensure the convergence of the DC-link voltage to its reference value (see Figs 13 and 15).

The various variation in refernce value (DC-voltage), have not affected the system stability (see Figs 10, 11 and 12). When varying the reference value, the super-capacitor operates either in charging mode or discharging mode (see Figs 13 and 16). The DC volatge is track to its reference values (see Fig 15). In addition, the super-capacitor current increases and decreases with load variation in order to ensure the power balance of the system (see Fig13).

The PI controller had a lower mean performance than the ISMC controller simulation results. The difference in

performance between the two controllers is more pronounced in the simulation, with the ISMC controller outperforming the PI controller by a larger margin. Overall, the results from the simulation are in good agreement with the experimental results, although there are some slight differences.

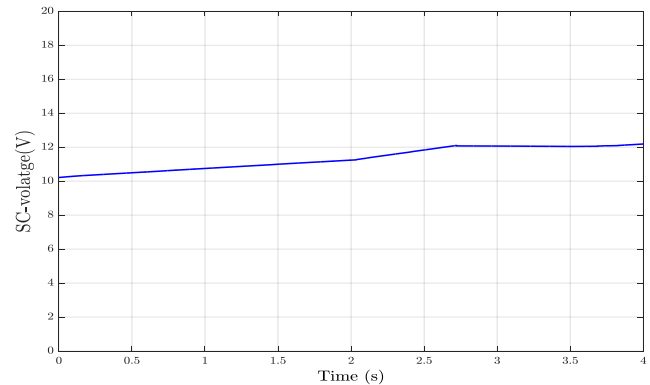


Fig. 10 – Experimental PV Volatge response (V).

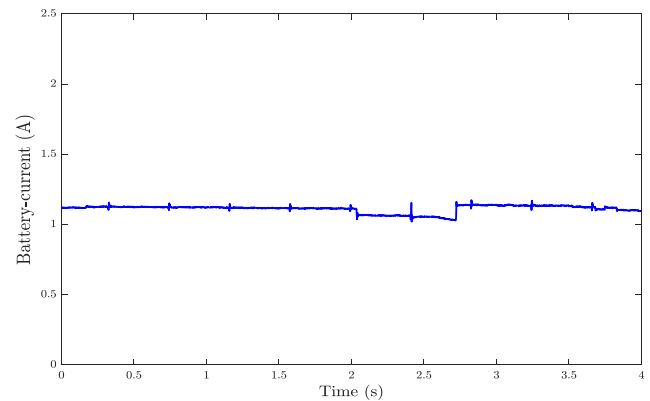


Fig. 11. Experimental battery current response (A)

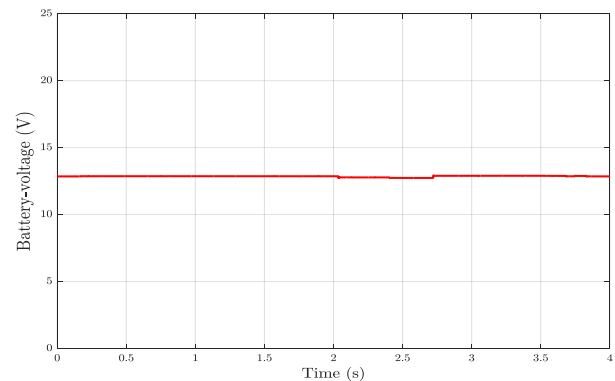


Fig. 12. Experimental battery voltage response (A)

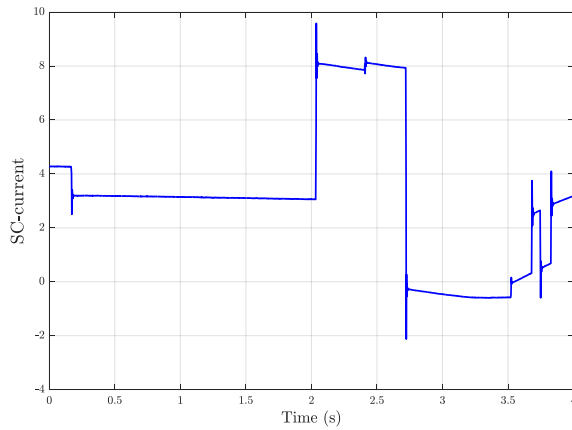


Fig. 13. Experimental current response of super-capacitor (A)

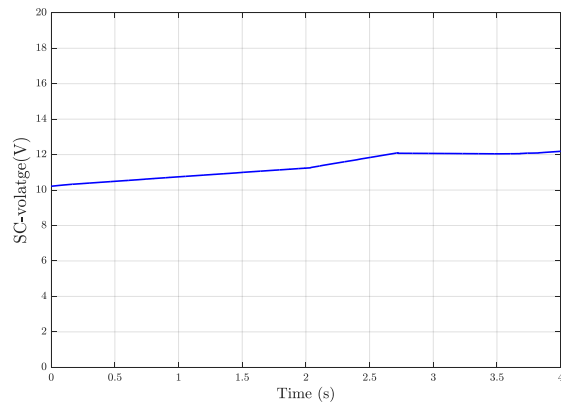


Fig. 14. Experimental voltage response of super capacitor (V).

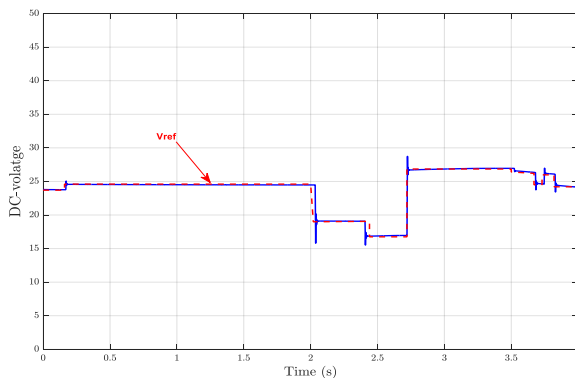


Fig. 15 – Experimental V_{DC} voltage (V).

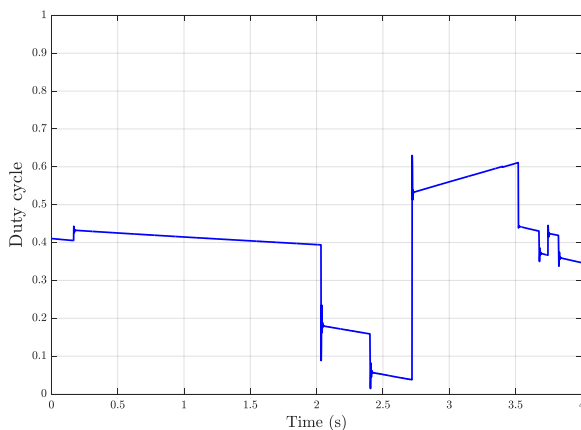


Fig. 16 – Experimental Duty-cycle for super-capacitor

6. CONCLUSIONS

Hybrid Energy Storage Systems (HESS) extend the life of batteries, minimizing the battery stress and enhancing the stability of hybrid systems thanks to the super-capacitor effect with a suitable control strategy. Super-capacitors in the HESS compensate for energy peaks, while batteries respond smoothly to irradiation changes, expanding their lifetime due to less aggressive power references.

This work proposes an ISMC-based nonlinear control strategy for a remote area power system consisting of HESS associated with a PV system. This control structure is based on high-frequency power and low decoupling, and it can regulate the DC-link at a constant value. The performance of this strategy control has been compared with PI-based linear control under the same irradiation change using simulation. Also, due to the linear behavior of the classical PI controller, the lack of a nonlinear controller may lead to less accurate setpoint tracking, and significant overshoot leads to reduce the lifespan of the battery. Finally, the obtained experimental and simulation results demonstrate the proposed controller exhibits better performance in terms of battery lifespan, ripples, and overshoot minimization.

Received 4 June 2022

7. REFERENCES

1. A. Attou, A., A. Massoum, M. Chadli, Comparison study of two tracking methods for photovoltaic systems, *Rev. Roum. Sci. Techn.–Électrotechn. et Énerg.*, 60, 2, pp. 205–214 (2015).
2. P.S. Sikder, P. Nital, Incremental conductance based maximum power point tracking controller using different buck-boost converter for solar photovoltaic system, *Rev. Roum. Sci. Techn.–Électrotechn. et Énerg.*, 62, 3, pp. 269–275 (2017).
3. B.K. Oubbati, M. Boutoubat, A. Rabhi, M. Belkheiri, “Experiential integral backstepping sliding mode controller to achieve the maximum power point of a PV system,” *Control Engineering Practice*, 102, p. 104570, Sep. 2020,
4. B. Yang et al., “Perturbation observer based fractional-order sliding-mode controller for MPPT of grid-connected PV inverters: Design and real-time implementation,” *Control Engineering Practice*, 79, pp. 105–125, Oct. 2018,
5. M. Jaszczur, Q. Hassan, “An optimisation and sizing of photovoltaic system with super-capacitor for improving self-consumption,” *Applied Energy*, 279, p. 115776, Dec. 2020,
6. S. Kotra, M.K. Mishra, “A supervisory power management system for a hybrid microgrid with HESS,” *IEEE Transactions on Industrial Electronics*, 64, 5, pp. 3640–3649, May 2017
7. U. Manandhar et al., “Energy management and control for grid connected hybrid energy storage system under different operating modes,” *IEEE Transactions on Smart Grid*, 10, 2, pp. 1626–1636, Mar. 2019.
8. L. W. Chong, Y.W. Wong, R.K. Rajkumar, D. Isa, “An optimal control strategy for standalone PV system with battery-super-capacitor hybrid energy storage system,” *Journal of Power Sources*, C, 331, pp. 553–565, Nov. 2016.
9. W. Jing, C.H. Lai, W.S.H. Wong, M.L.D. Wong, “A comprehensive study of battery-super-capacitor hybrid energy storage system for standalone PV power system in rural electrification,” *Applied Energy*, 224, pp. 340–356, Aug. 2018,
10. S.K. Kollimalla, M.K. Mishra, L.N.N., “A new control strategy for interfacing battery supercapacitor storage systems for PV system,” 2014. Accessed: Apr. 21, 2022. [Online]. Available: <https://ieeexplore.ieee.org/document/6804478/>
11. B.R. Ravada, N.R. Tummuru, “Control of a supercapacitor-battery-PV based stand-alone dc-microgrid,” *IEEE Transactions on Energy Conversion*, 35, 3, 2020, HESS, Accessed: Apr. 21,